

Mode Analytical Study of Cylindrical Cavity Power Combiners

KIYOSHI FUKUI, MEMBER, IEEE, AND SHIGEJI NOGI

Abstract — A mode analytical treatment of cylindrical cavity power combiners is presented to discuss power-combining capability and the method for attaining stable desired mode operation. Both the conventional coaxial-probe output type and the window output type are treated, based on a circuit model which can support TM_{010} , TM_{020} , and TM_{m10} modes ($1 \leq m \leq N$, N being the number of active devices employed). It is shown that adoption of the window output largely facilitates undesired mode suppression and also enables power combining in some azimuthal modes.

I. INTRODUCTION

RECENTLY, TO meet the demands for high-power microwave sources, various power-combining techniques have been developed [1], [2]. Among them, the resonant cavity combiner has been actively studied by many authors. To this category belong the waveguide cavity combiners first proposed by Kurokawa and Magalhaes [3]–[9] and the cylindrical cavity combiners originated by Harp and Stover [10]–[14]. While the latter has excellent features in its small size and symmetrical geometry, practicability in the millimeter-wave range is less likely than in the microwave region because the modeling problem becomes serious if the cavity diameter is increased to accommodate more diodes. It is also said that accurate fabrication of a coaxial output probe becomes difficult at high frequencies, resulting in deterioration of performances [2].

The most fundamental and important problems in the discussion of a multiple-device cavity combiner are its power-combining capability and stability of operation in a desired mode. In a recent paper [14], the authors presented a theoretical work concerning these problems for a cylindrical cavity multiple-device oscillator by discussing the competitive relations between the desired power-combining mode and stable undesired modes. Such an approach is beneficial in finding efficient combiner structures which facilitate undesired mode suppression. For example, the use of a window output structure (Fig. 1) is advantageous in making mode control easy (see later sections). This structure will also give a solution to the problem of manufacturability in the millimeter-wave region.

This paper presents a unified-mode analytical treatment of cylindrical cavity combiners both with a probe output

Manuscript received October 28, 1985; April 28, 1986. This work was supported in part by a Grant in Aid for Fundamental Research from the Ministry of Education, Japan.

The authors are with the Department of Electronics, Okyama University, Okyama 700, Japan.

IEEE Log Number 8609604.

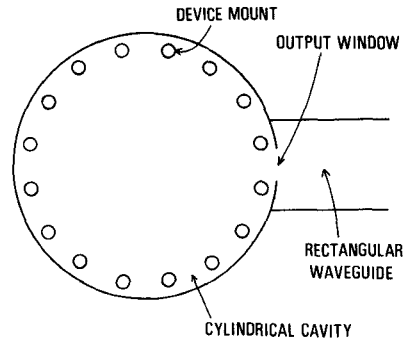


Fig. 1. Window output cylindrical cavity combiner (top view).

and with a window output. For each combiner structure, the power-combining modes and stable undesired modes are derived by use of the averaged potential theory [15]. A comparison of the two structures on the feasibility of mode control for the stable desired mode operation is given.

II. CIRCUIT MODEL AND ITS NORMAL MODES

A. Circuit Model and Basic Equations

To render the problems amenable to analytical treatment, we introduce a circuit model of a cylindrical cavity combiner with N active devices shown in Fig. 2.¹ The current–voltage characteristic of the devices is assumed as

$$J_k = -gv_k + \frac{4}{3}\theta v_k^3 \quad 1 \leq k \leq N. \quad (1)$$

The load conductance g_L is connected to the center for the probe output type as shown in the figure, and to site 1 on the periphery for the window output type. In order for the circuit model to be adequate for our purposes, it is necessary that 1) the network without J_k 's and g_L , which we call the generating system, supports all the relevant cavity modes, and 2) coupling of the devices with the cavity field can be described. The model of Fig. 2 fulfills the second requirement because, if there exists any oscillation in the generating system, the voltages v_k 's act on the devices whose active nonlinear currents in turn excite the oscillation. For the first requirement stated above, detailed discussions are given in Section II-B.

¹For a discussion of the conventional coaxial-probe output type only, we can use a simpler model which contains only N device sites and the center (load position) [14].

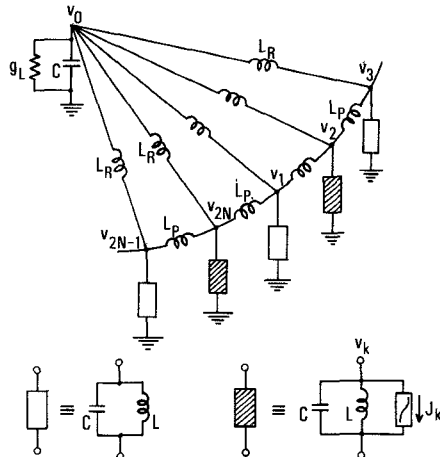


Fig. 2. Circuit model of a cylindrical cavity combiner (for window output type, g_L is placed at the site 1 on the periphery).

where

$$\epsilon = \frac{g}{\omega_0 c} \quad \epsilon_L \frac{g_L}{\omega_0 C} \quad (4)$$

and

$$\beta_P = L/L_P \quad \beta_R = L/L_R. \quad (5)$$

B. Normal Modes

Consider the generating system of the circuit model to define the normal modes. Putting the right side in each of (3) zero, the generating system is expressed by the following vector differential equation:

$$\frac{d^2 v}{d\tau^2} + Bv = 0 \quad (6a)$$

with

$$v = [v_0, v_1, \dots, v_{2N}]^t \quad (6b)$$

and

$$B = \begin{bmatrix} 2N\beta_R & -\beta_R & -\beta_R & \dots & -\beta_R \\ -\beta_R & 1+2\beta_P+\beta_R & -\beta_P & \dots & -\beta_P \\ -\beta_R & -\beta_P & \dots & \dots & -\beta_P \\ \vdots & \vdots & \ddots & \ddots & \vdots \\ -\beta_R & 0 & -\beta_P & \dots & -\beta_P \\ & & & \ddots & 1+2\beta_P+\beta_R \end{bmatrix}. \quad (6c)$$

Additionally, for the discussion of the output power of the system and the stability of the modes, only the voltage values at the $N+1$ positions (N device positions plus one load position) are needed, whatever detailed circuit model having many more lattice points² may be used [14]. Thus, the circuit model as shown here is considered to be an appropriate model whose behavior is analogous to the actual cylindrical cavity combiner.

Using a new time variable

$$\tau = \omega_0 \tau, \quad \omega_0 = \sqrt{LC} \quad (2)$$

the governing equations of the circuit model are written as

$$\begin{aligned} \frac{d^2 v_0}{d\tau^2} + \beta_R \sum_{k=1}^{2N} (v_0 - v_k) \\ = \begin{cases} -\epsilon_L \frac{dv_0}{d\tau} & \text{for central loading} \\ 0 & \text{for peripheral loading} \end{cases} \end{aligned} \quad (3a)$$

$$\begin{aligned} \frac{d^2 v_1}{d\tau^2} + (1+2\beta_P+\beta_R)v_1 - \beta_P(v_{2N} + v_2) - \beta_R v_0 \\ = \begin{cases} 0 & \text{for central loading} \\ -\epsilon_L \frac{dv_1}{d\tau} & \text{for peripheral loading} \end{cases} \end{aligned} \quad (3b)$$

$$\begin{aligned} \frac{d^2 v_k}{d\tau^2} + (1+2\beta_P+\beta_R)v_k - \beta_P(v_{k-1} + v_{k+1}) - \beta_R v_k \\ = \frac{\epsilon}{2} \left\{ 1 + (-1)^k \right\} \left(1 - 4 \frac{\theta}{g} v_k^2 \right) \frac{dv_k}{d\tau}, \quad 2 \leq k \leq 2N \end{aligned} \quad (3c)$$

²A lattice model is often used for two-dimensional distributed-constant systems.

Then, the normal modes can be defined if the eigenvalues ω_i^2 's and the eigenvectors p_i 's are obtained by solving

$$Bp_i = \omega_i^2 p_i, \quad 0 \leq i \leq 2N \quad (7a)$$

with

$$p_i = [p_{0i}, p_{1i}, \dots, p_{2N,i}]^t. \quad (7b)$$

The results are given below, where

$$p_i^t \cdot p_j = \delta_{ij}, \quad 0 \leq i, j \leq 2N \quad (8)$$

is imposed.

1) $i = 0, 1$:

$$\omega_i^2 = \frac{1}{2} \left\{ 1 + \beta_R + 2N\beta_R \mp \sqrt{(1 + \beta_R - 2N\beta_R)^2 + 8N\beta_R^2} \right\} \quad (9)$$

$$p_{ki} = \begin{cases} c_{\pm} p_{\pm}, & k = 0 \\ p_{\pm}, & 1 \leq k \leq 2N \end{cases} \quad (10a)$$

where

$$c_{\pm} = \frac{1}{2\beta_R} \left\{ 1 + \beta_R - 2N\beta_R \pm \sqrt{(1 + \beta_R - 2N\beta_R)^2 + 8N\beta_R^2} \right\}$$

$$p_{\pm}^2 = (c_{\pm}^2 + 2N)^{-1}. \quad (10b)$$

In the double signs appearing in (9) and (10), the upper

and lower signs correspond to $i = 0$ and $i = 1$, respectively.

2) $2 \leq i \leq 2N$:

$$\begin{aligned} \omega_i^2 &= 1 + \beta_R + 4\beta_P \sin^2 \frac{\pi(i-1)}{2N} \\ p_{0i} &= 0 \end{aligned} \quad (11)$$

$$\begin{aligned} p_{ki} &= \begin{cases} \sqrt{\frac{1}{N}} \cos \frac{\pi(k-1)(i-1)}{N}, & 2 \leq i \leq N \\ (-1)^k \sqrt{1/2N}, & i = N+1 \\ \sqrt{\frac{1}{N}} \sin \frac{\pi(k-1)(i-1)}{N}, & N+2 \leq i \leq 2N \end{cases} \\ & \quad (12) \end{aligned}$$

The two modes i and $\tilde{i} = 2N+2-i$ are degenerate to each other because

$$\omega_i = \omega_{\tilde{i}}, \quad \tilde{i} = 2N+2-i \quad (13)$$

is obtained from (11). The number of the degenerate-mode pairs is $N-1$, and the spatial patterns of a pair differ only in phase by $\pi/2$ along the periphery.

We give here a brief comment on the correspondence between the normal modes of the circuit model and the resonant modes in the original cavity. First, mode 0 and mode 1 correspond, respectively, to the TM_{010} and TM_{020} modes because they have constant amplitude distribution at the periphery and the oscillation at the center is, respectively, inphase and antiphase with the oscillation at the periphery.

Next, mode i ($2 \leq i \leq N$) and mode $\tilde{i} = 2N+2-i$ ($N+2 \leq \tilde{i} \leq 2N$) have zero amplitude at the center and $i-1$ times sinusoidal variation along azimuthal direction, so these correspond to the $\text{TM}_{i-1,1,0}$ mode. Similarly, the remaining mode $N+1$ corresponds to the TM_{N10} mode. In the later sections, mode i 's ($2 \leq i \leq 2N$) are referred to as "ring" modes or "azimuthal" modes.

Thus, the circuit model of Fig. 2 can support only the $N+2$ cavity modes TM_{010} , TM_{020} , and $\text{TM}_{i-1,1,0}$ ($2 \leq i \leq N+1$). However, these modes will be sufficient for the discussion in this paper because the frequency range of active devices is limited. In addition, from a more practical standpoint, as long as mode 0 or mode 1 is chosen as the desired power-combining mode and N is taken as $N > 8$, the modes $N/2+1 \leq i \leq 3N/2$ are often out of the relevant frequency range, so these modes can be omitted when simplicity of description is desired.

III. AVERAGED POTENTIAL AND POWER-COMBINING MODES

A. Averaged Potential

According to the averaged potential theory [15], the time evolution of a system proceeds toward the direction of decreasing value of the averaged potential of the system, and the stationary states correspond to the minimum points

of the quantity.³ For our system, it is composed of two parts: the contribution from active devices U_D , and that from the load U_L . They are defined as follows:

$$\begin{aligned} U_D &= \text{time average of } \sum_k \int J_k dv_k \\ U_L &= \text{time average of } \int g_L v_l dv_l \end{aligned} \quad (14)$$

where v_l stands for v_0 or v_1 depending on whether central loading or peripheral loading is considered.

Using (1) and the normal-mode expansion of v_k

$$v_k = \sum_{i=0}^{2N} p_{ki} A_i \cos(\omega_i \tau + \phi_i), \quad 0 \leq k \leq 2N \quad (15)$$

we can express the averaged potential of the system as

$$\begin{aligned} 4U &= - \sum_{i=0}^{2N} \alpha_i A_i^2 + \frac{1}{2} \sum_{i=0}^{2N} \sum_{j=0}^{2N} \theta_{ij} A_i^2 A_j^2 \\ &+ \frac{1}{2} \sum_{i=2}^N \theta_{ii} A_i^2 A_i^2 \cos 2\psi_i \\ &+ 8 \sum_{i=2}^N \sum_{j=2}^N \xi_{i\tilde{i}j\tilde{j}} A_i A_{\tilde{i}} A_j A_{\tilde{j}} \cos \psi_i \cos \psi_j \end{aligned} \quad (16)$$

where (see Appendix I)

$$\alpha_i = g \sum_{k: \text{even}} p_{ki}^2 - g_L p_{li}^2 \quad (17)$$

$$p_{li} = \begin{cases} p_{0i} & \text{for central loading} \\ p_{1i} & \text{for peripheral loading} \end{cases} \quad (18)$$

$$\theta_{ij} = (2 - \delta_{ij}) \theta \sum_{k: \text{even}} p_{ki}^2 p_{kj}^2 \quad (19)$$

$$\xi_{i\tilde{i}j\tilde{j}} = \theta \sum_{k: \text{even}} p_{ki} p_{\tilde{k}i} p_{kj} p_{\tilde{k}j} \quad (20)$$

and

$$\psi_i = \phi_i - \phi_{\tilde{i}}. \quad (21)$$

α_i is a small-signal gain parameter of mode i ; the amplitude of mode i grows as $\exp[\alpha_i \tau]$, as long as all the modes are at low level. θ_{ii} and θ_{ij} ($i \neq j$) are called self- and mutual-saturation parameters, respectively, and their magnitudes depend on the degree of spatial correlation between the relevant modes. $\xi_{i\tilde{i}j\tilde{j}}$ has a similar meaning to θ_{ij} , except that modes i and j are replaced by degenerate-mode pairs (i, \tilde{i}) and (j, \tilde{j}) , respectively.

By substitution of (10) and (12) into (17)–(20), these parameters can be evaluated. α_i depends on the value of g_L , and will be given after determining the latter in Section III-B. The expressions of θ_{ij} 's and $\xi_{i\tilde{i}j\tilde{j}}$'s are a little lengthy, so their full extent is given in Appendix II. But a simpler expression for θ_{ij} 's is given in the following matrix form for a reduced number of modes, discarding the modes $1+N/2, \dots, 3N/2$ as mentioned at the end of

³By this, the approach using the averaged potential, which gives an approximation of the same order as in the averaging method [16], largely simplifies the discussion of stability of the stationary states.

Section II-B:

$$\left[\theta_{ij}/\theta \right] = \begin{bmatrix} Np_+^4 & 2Np_+^2 p_-^2 & p_+^2 & \cdots & p_+^2 & 2p_+^2 & p_+^2 & \cdots & p_+^2 \\ 2Np_+^2 p_-^2 & Np_-^4 & p_-^2 & \cdots & p_-^2 & 2p_-^2 & p_-^2 & \cdots & p_-^2 \\ p_+^2 & p_-^2 \\ \vdots & \vdots \\ p_+^2 & p_-^2 \\ 2p_+^2 & 2p_-^2 \\ p_+^2 & p_-^2 \\ \vdots & \vdots \\ p_+^2 & p_-^2 \end{bmatrix}' \quad \begin{matrix} i = 0 \\ 1 \\ 2 \\ \vdots \\ N/2 \\ 3N/2+1 \\ \vdots \\ 2N \end{matrix} \quad (22a)$$

All the elements left blank must be filled out with 2, except the common factor $1/4N$. In (22a) and (22b), mode numbers are given on the right of the matrix for reference.

B. Power-Combining Modes

Consider a steady state in which only one mode, say mode i , is excited. The amplitude of steady oscillation at this mode is determined by solving $\delta U / \delta A_i^2|_{A_i \neq 0, \text{others}=0} = 0$ as

$$A_i^2 = \alpha_i / \theta_i \equiv A_{i0}^2. \quad (23)$$

The output power in this state $P(l, i)$, where l takes 0 for the case of central loading and 1 for the case of peripheral loading, is then given by

$$P(l, i) = \frac{1}{2} g_L p_{li}^2 A_i^2 = \frac{1}{2} g_L p_{li}^2 \alpha_i / \theta_{ii}. \quad (24)$$

g_L is chosen so as to maximize $p(l, i)$ and the optimum value is denoted as $g_{L_{\text{opt}}}(l, i)$.

In the case of central loading, $p_{li} = p_{0i}$ has a nonvanishing value only for mode 0 and mode 1. The maximum output power for these two modes and the corresponding

optimum load conductances are given as

$$P_{\max}(0, i) = \frac{Ng^2}{8\theta}, \quad i = 0, 1 \quad (25)$$

$$g_{L,\text{opt}}(0, i) = \begin{cases} Ng/(2c_+)^2, & i = 0 \\ Ng/(2c_-)^2, & i = 1 \end{cases}. \quad (26)$$

Since the available power of an active device having the current-voltage characteristic of (1) is given by $g^2/(8\theta)$ [5], it can be seen in (25) that perfect power combining of all the available powers is possible either in mode 0 or in mode 1.

For peripheral loading, $p_{1t} = p_{1i} \neq 0$ for the modes $0, 1, 2, \dots, N+1$, so, we obtain the maximum output power at mode i ($0 \leq i \leq N+1$)

$$p_{\max}(1, i) = \frac{g^2}{8\theta_{i_1}} \left(\sum_{k: \text{even}} p_{ki}^2 \right)^2$$

for

$$g_L = \frac{g}{p_{1l}^2} \sum_{k: \text{even}} p_{k1}^2$$

which gives, using (10) and (12)

$$P_{\max}(1, i) = \begin{cases} \frac{Ng^2}{8\theta}, & i = 0, 1, \frac{N}{4} + 1, \frac{3N}{4} + 1, N + 1 \\ \frac{Ng^2}{12\theta}, & 2 \leq i \leq N \quad (i \neq \frac{N}{4} + 1, \frac{3N}{4} + 1) \end{cases} \quad (27)$$

Thus, the peripheral-loading system has three power-combining ring modes other than mode 0 and mode 1, as indicated in (27). The optimum load conductances for the power-combining modes are

$$g_{L,\text{opt}}(1, i) = \begin{cases} \frac{1}{2}Ng, & i = 0, 1, N + 1 \\ \frac{1}{4}Ng, & i = \frac{N}{4} + 1, \frac{3N}{4} + 1 \end{cases} \quad (28)$$

In the following, we adopt mode 1 as the desired power-combining mode both for central and peripheral loading. Then, using $g_{L,\text{opt}}(1, 1)$, the gain parameters can be determined as

$$\alpha_i(l=0) = \begin{cases} (N/2)(2 - c_+^2/c_-^2)p_+^2g, & i = 0 \\ (N/2)p_-^2g, & i = 1 \\ \frac{1}{2}g, & 2 \leq i \leq 2N \\ 0, & i = N/2 + 1 \\ g, & i = 3N/2 + 1 \end{cases} \quad (i = N/2 + 1, 3N/2 + 1) \quad (29)$$

for the central-loading system, and

$$\alpha_i(l=1) = \begin{cases} (N/2)p_+^2g, & i = 0 \\ (N/2)p_-^2g, & i = 1 \\ 0, & 2 \leq i \leq N \quad (i \neq N/2 + 1) \\ -\frac{1}{2}g, & i = N/2 + 1 \\ \frac{1}{4}g, & i = N + 1 \\ \frac{1}{2}g, & N + 2 \leq i \leq 2N \quad (i \neq 3N/2 + 1) \\ g, & i = 3N/2 + 1 \end{cases} \quad (30)$$

for the peripheral-loading system. Then, the mode $N/2 + 1$ in the central-loading system and the modes $2, 3, \dots, N$ in the peripheral-loading system can be put out of consideration because their α_i values are zero or negative, which means there is no possibility of oscillation. Note that the peripheral-loading system has more nonoscillatory modes than the central-loading system.

IV. STABILITY OF THE MODES

A. Stability Conditions

Now, we must ask if the desired power-combining mode can be stable and how many and what type of undesired stable modes exist in our power-combiner system.

Stability conditions can be derived from the criterion of the averaged potential minimum. First, for the stability of a single mode, say mode i , the criterion gives

$$\left. \frac{\partial U}{\partial A_d^2} \right|_{A_i = A_{i0}, \text{all others} = 0} = -\alpha_d + (1 - \frac{1}{2}\delta_{di})\theta_{di}A_{i0}^2 > 0, \quad \text{for all } d \neq i. \quad (31)$$

This means that the steady-state oscillation at mode i makes the growth of all the other modes impossible.

Next, in order for mode i and mode j to form a stable simultaneous double-mode oscillation, the following two conditions must be satisfied. They are

$$\begin{vmatrix} \theta_{ii} & (1 - \frac{1}{2}\delta_{ji})\theta_{ij} \\ (1 - \frac{1}{2}\delta_{ji})\theta_{ij} & \theta_{jj} \end{vmatrix} > 0 \quad (32)$$

and

$$\begin{aligned} \left. \frac{\partial U}{\partial A_d^2} \right|_{A_i = A_{is}, A_j = A_{js}, \text{others} = 0} &= -\alpha_d + (1 - \frac{1}{2}\delta_{di})\theta_{di}A_{is}^2 \\ &+ (1 - \frac{1}{2}\delta_{dj})\theta_{dj}A_{js}^2 > 0, \quad \text{for all } d \neq i, j. \end{aligned} \quad (33)$$

A_{is} and A_{js} are the steady-state amplitudes of both modes, and can be obtained from

$$\begin{aligned} \left. \frac{\partial U}{\partial A_i^2} \right|_{A_i, A_j \neq 0, \text{others} = 0} &= \left. \frac{\partial U}{\partial A_j^2} \right|_{A_i, A_j \neq 0, \text{others} = 0} = 0 \\ \frac{\partial U}{\partial \psi_i} = 0 \quad \text{with} \quad \frac{\partial^2 U}{\partial \psi_i^2} > 0 \quad \text{for } j = \tilde{i}. \end{aligned}$$

Condition (32) is necessary for the coexistence of both modes. Equation (33) has a similar meaning of that of (31), that is, other modes never grow due to the existence of the double-mode oscillation.

B. Stable Modes

By use of the stability conditions given above, the stable modes are derived both for the central loading and for the peripheral loading. The results are listed in Table I. The modes 0 and 1 are quasi-stable, as will be discussed shortly, and do not enter the table. No simultaneous multimode oscillations with higher multiplicity exist either for the central loading or for the peripheral loading because we cannot find any mode groups in which every pair of two component modes satisfies the coexistence condition (32). It should be noted that many of the stable modes in the central-loading case turn to unstable modes in the case of peripheral loading. This is because, in the latter, the load on the periphery serves to raise the averaged potential of many ring modes.

Common features in the stable modes can be expressed as follows. i) every active device can oscillate at equal (or almost equal) amplitude, as seen in Fig. 3, where the mode patterns are shown in developed form for the case $N = 8$. The degenerate double mode (i, \tilde{i}) in the central-loading

TABLE I
LIST OF STABLE MODES

stable mode	mode number	squared amplitude	averaged potential
single-mode	$\nu N/4+1$ ($\nu=1, 3$)	$2Ng/\theta$	$-Ng^2/80$
	$N+1$	$2Ng/\theta$	$-Ng^2/80$
	$3N/2+1$	Ng/θ	$-Ng^2/80$
degenerate double-mode	$\nu N/4+1$ ($\nu=5, 7$)	$2Ng/\theta$	$-Ng^2/80$
	i, \tilde{i} $2 \leq i \leq N$ $i \neq N/4+1$ ($\nu=1, 2, \dots, 7$)	$\frac{Ng}{\theta}, \frac{Ng}{\theta}$	$-\frac{Ng^2}{80}$
	$(N/4+1-n) (N/4+1+n)^*$ $(3N/4+1+n), (3N/4+1-n)$	$\frac{4Ng}{50}, \frac{4Ng}{50}$	$-\frac{Ng^2}{100}$
non-degenerate double-mode	$(5N/4+1-n) (5N/4+1+n)$ $(7N/4+1+n), (7N/4+1-n)$ $n=1, \dots, N/4-1$	$\frac{4Ng}{50}, \frac{4Ng}{50}$	$-\frac{Ng^2}{100}$

For the peripheral-loading case, only the parts framed by the bold lines are applicable.

* $\binom{a}{b}, \binom{c}{d}$ stand for any mode pair of $(a, c), (a, d), (b, c)$, and (b, d) .

case forms a rotating wave around the center because $\psi_i = \pm \pi/2$, and this enables all the active devices to oscillate with exactly equal amplitude. ii) Oscillation amplitude at the load is zero in all the stable modes, which makes U_L zero, the minimum contribution to the averaged potential from the load part.

The desired mode (mode 1), which satisfies only item i) and has the averaged potential of $-Ng^2/32\theta$, is quasi-stable because the left side of (31) is zero for some of the ring modes. Thus, some plans are needed to stabilize the desired mode and to make all the undesired modes unstable.

V. UNDESIRED MODE SUPPRESSION

Let us now proceed to the problem of stabilization of the desired mode and simultaneous destabilization of undesired modes. Since mode 0 (TM_{010} mode) and assuming $N \geq 10$, mode $N+1$ (TM_{N10} mode) are far enough separated in frequency from the desired mode (TM_{020} mode), usually they are not excited at all because of the limited working range of currently available diodes and, in case of necessity, they can easily be suppressed by use of coaxial modules [1]. So, in the following, we confine ourselves to discussion of the suppression of all the remaining undesired modes, that is, modes $2 \leq i \leq 2N$ except $i = N+1$.

We introduce conductances g_{sp} 's for absorbing undesired azimuthal modes in the way as shown in Fig. 4. These contribute to raise the averaged potential for undesired modes without any effect on the desired mode. The increment of the averaged potential ΔU , due to introduction of a conductance g_{sp} between two neighboring device sites, say k th and $(k+2)$ th, is given, by calculating the time average of $\int g_{sp} (v_{k+2} - v_k) d(v_{k+2} - v_k)$, as

$$\Delta U = - \sum_{i=0}^{2N} \Delta \alpha_i A_i^2 - \sum_{i=2}^N \Delta \alpha_{ii} A_i A_{\tilde{i}} \cos \phi_i \quad (34)$$

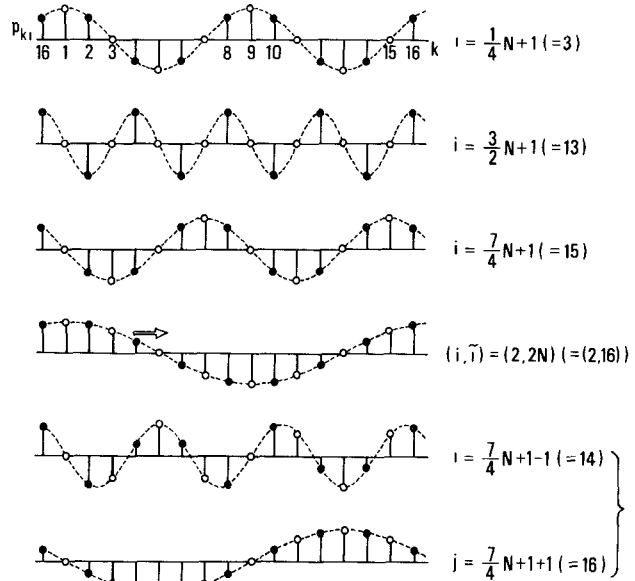


Fig. 3. Spatial patterns of some typical stable modes ($N = 8$). Closed circles refer to the amplitudes at the sites of active devices. Note that the last two modes, $i = 7N/4$ and $j = 7N/4+2$, make mutual concessions at the device sites to form a stable nondegenerate double mode.

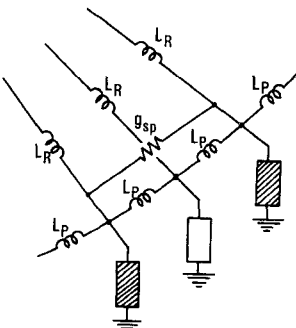


Fig. 4. Introduction of g_{sp} for suppression of undesired azimuthal modes.

with

$$\begin{aligned} \Delta \alpha_i &= -g_{sp}(p_{k+2,i} - p_{k,i})^2 \\ \Delta \alpha_{ii} &= -2g_{sp}(p_{k+2,i} - p_{k,i})(p_{k+2,\tilde{i}} - p_{k,\tilde{i}}). \end{aligned} \quad (35)$$

When more than two pieces of g_{sp} are used, summation over k must be made on the right sides in (35).

A. Case of Central Loading

First, in the case of a central-loading system, use of a single g_{sp} has almost no effect on the suppression of the azimuthal modes. The reason is as follows. Linear combination of modes $i = N/4+1$ and $\tilde{i} = 7N/4+1$ (or modes $i = 3N/4+1$ and $\tilde{i} = 5N/4+1$) can result in any azimuthal shift of the spatial pattern of mode i (or mode \tilde{i}). Then, when a single g_{sp} is introduced, the mode pair (i, \tilde{i}) forms a standing-wave pattern such that the voltages at both ends of g_{sp} are equal to each other and can escape from damping. Also, the mode pairs (i, \tilde{i}) which appear as rotating-wave double modes in the absence of g_{sp} behave in the same way and cannot be suppressed. Then, at least

two pieces of g_{sp} are necessary for suppression of these modes. Since the optimum way of introducing two g_{sp} 's is different from mode to mode to be suppressed, we consider the case in which every pair of neighboring device sites are connected by g_{sp} . In this case, $\Delta\alpha_i$ and $\Delta\alpha_{i\tilde{i}}$ become

$$\Delta\alpha_i = \begin{cases} 0, & i = 0, 1, N+1 \\ -2g_{sp} \sin^2 \frac{(i-1)\pi}{N}, & \text{otherwise} \end{cases}$$

$$\Delta\alpha_{i\tilde{i}} = 0. \quad (36)$$

In order that any degenerate double mode (i, \tilde{i}) is unstable to permit the growth of the desired mode, the following condition must be satisfied:

$$\alpha_1 - \theta_{1i} A_{is}^2 - \theta_{1\tilde{i}} A_{i\tilde{i}s}^2 > 0 \quad \text{for } 2 \leq i \leq N \quad (37)$$

which is obtained by putting $d=1$ and reversing the inequality sign in (33). In (37), A_{is} and $A_{i\tilde{i}s}$ are the steady-state amplitudes after introduction of g_{sp} 's. It follows from (37) that

$$g_{sp} > \frac{3}{16} g \operatorname{cosec}^2 \frac{(i-1)\pi}{N} \quad \text{for } 2 \leq i \leq N$$

for the suppression of the double mode (i, \tilde{i}) . The double mode most difficult to suppress is $(i, \tilde{i}) = (2, 2N)$. Consequently, the necessary and sufficient conditions for suppression of all the azimuthal modes is given, denoting g_{sp} as $g_{sp, \text{centr}}$, by

$$Ng_{sp, \text{centr}} > \frac{3}{16} Ng \operatorname{cosec}^2 \frac{\pi}{N}. \quad (38)$$

The factor N on both sides means that N pieces are being used.

B. Case of Peripheral Loading

Next, in the case of the peripheral-loading system, all the modes $i \leq N$ have no possibility of excitation because $\alpha_i \leq 0$ due to the load on the periphery. Thus, the system has no stable degenerate double modes, which largely facilitates the mode control. Since all the modes to be suppressed have the largest voltage difference at the interval $k = N$ and $k = N+2$, placing of one piece of g_{sp} at this interval must be most efficient for suppression. The condition of suppression is given, this time, by

$$\alpha_1 - \theta_{1i} A_{i0}^2 > 0 \quad \text{for } N+2 \leq i \leq 2N \quad (39)$$

which is obtained by putting $d=1$ and reversing the inequality sign in (31), and in which $A_{i0}^2 = (\alpha_i + \Delta\alpha_i)/\theta_{ii}$. The required g_{sp} value then becomes, denoting g_{sp} as $g_{sp, \text{periph}}$

$$g_{sp, \text{periph}} > \frac{5}{64} Ng \operatorname{cosec}^2 \frac{\pi}{N}. \quad (40)$$

Let us now compare both the loading systems concerning the feasibility of undesired mode suppression. By comparing (40) with (38), it is seen that adoption of the peripheral loading largely facilitates the undesired mode suppression, both in number and in the total quantity of g_{sp} 's required. From the practical side, the latter point will

be important in view of possible power loss due to g_{sp} 's in the desired mode. Incidentally, if N pieces of g_{sp} are used in the same manner as in the central-loading case, the necessary g_{sp} value is given by $Ng_{sp} > (5/32)Ng \operatorname{cosec}^2(\pi/N)$.

VI. CONCLUSIONS

A mode analytical study has been carried out on the power-combining behavior of cylindrical cavity multiple-device structures in the TM_{020} mode, based on a circuit model which can support TM_{010} , TM_{020} , and TM_{m10} modes ($1 \leq m \leq N$). Both the conventional coaxial-probe output type and the window output type have been treated and it has been shown that the latter is preferable for undesired mode suppression. The analysis developed in this paper is useful not only for understanding the power-combining mechanism and multimode behavior of the structures, but also for finding effective methods or favorable structures for undesired mode suppression. For example, nonuniform arrangements of devices will be advantageous for the mode control in the case of a relatively small number of undesired modes to be suppressed. Experimental works on window output structures are highly desired to confirm the theory and to develop further possibilities, although some successful results have already been obtained [17].

As described in Section III, the window output cylindrical cavity can be employed also as a power combiner at azimuthal modes such as $\text{TM}_{N/4,1,0}$, which may be favorable for use in the millimeter-wave region because of large size for N properly chosen. Investigation of this case would also be an interesting subject for further work.

APPENDIX I DERIVATION OF (16)

Substitution of (1) into (14) gives

$$U_D = -\frac{1}{2} g \sum_{k: \text{even}} V_k^2 + \frac{1}{3} \theta \sum_{k: \text{even}} V_k^4$$

$$U_L = \frac{1}{2} g_L V_l^2 \quad (l = 0 \text{ or } 1) \quad (41)$$

where V_k^2 and V_k^4 are the time average of v_k^2 and v_k^4 , respectively. Using (15) for v_k and putting $\psi_i = \phi_i - \phi_{i\tilde{i}}$, we obtain

$$V_k^2 = \frac{1}{2} \sum_{i=0}^{2N} p_{ki}^2 A_i^2 + \sum_{i=2}^N p_{ki} p_{k\tilde{i}} A_i A_{\tilde{i}} \cos \psi_i \quad (42a)$$

$$V_k^4 = \frac{3}{8} \sum_{i=0}^{2N} \sum_{j=0}^{2N} (2 - \delta_{ij}) p_{ki}^2 p_{kj}^2 A_i^2 A_j^2$$

$$+ \frac{3}{4} \sum_{i=2}^N p_{ki}^2 p_{k\tilde{i}}^2 A_i^2 A_{\tilde{i}}^2 \cos 2\psi_i$$

$$+ 6 \sum_{i=2}^N \sum_{j=2}^N p_{ki} p_{k\tilde{i}} p_{kj} p_{k\tilde{j}} A_i A_{\tilde{i}} A_j A_{\tilde{j}} \cos \psi_i \cos \psi_j$$

$$+ \text{terms which vanish if summed up over even } k \text{ 's.} \quad (42b)$$

Substitution of (42) into (41) and use of the relations

$$\begin{aligned} \sum_{k: \text{ even}} p_{ki} p_{k\tilde{i}} &= \sum_{k: \text{ even}} p_{ki}^3 p_{\tilde{i}} \\ &= \sum_{k: \text{ even}} p_{ki}^2 p_{kj} p_{k\tilde{j}} = 0 \end{aligned} \quad (43)$$

gives the expression for U_D .

For V_l^2 ($l = 0, 1$), the second term vanishes in (42a) because $p_{li} p_{l\tilde{i}} = 0$. So, we have directly

$$U_L = \frac{1}{4} g_L \sum_{i=0}^{2N} p_{ii}^2 A_i^2. \quad (44)$$

Summation of U_D and U_L and the use of notations (17) ~ (20) leads to the final expression (16).

ACKNOWLEDGMENT

The authors wish to thank T. Kishimoto for his great help in carrying out the calculations concerning the mode analysis.

REFERENCES

- [1] K. J. Russell, "Microwave power combining techniques," *IEEE Trans. Microwave Theory Tech.*, vol. MTT-27, pp. 472-478, May 1979.
- [2] K. Chang and C. Sun, "Millimeter-wave power-combining techniques," *IEEE Trans. Microwave Theory Tech.*, vol. MTT-31, pp. 91-107, Feb. 1983.
- [3] K. Kurokawa and F. M. Magalhae, "An X-band 10-W multiple-diode oscillator," *Proc. IEEE*, vol. 59, pp. 102-103, Jan. 1971.
- [4] K. Kurokawa, "The single-cavity multiple-device oscillator," *IEEE Trans. Microwave Theory Tech.*, vol. MTT-19, pp. 793-801, Oct. 1971.

APPENDIX II

EXPRESSIONS FOR θ_{ij} 'S AND $\xi_{i\tilde{i}j\tilde{j}}$ 'S

$$\frac{\theta_{ij}}{\theta} = \begin{cases} Np_+^4 & \text{for } i = j = 0 \\ Np_-^4 & \text{for } i = j = 1 \\ 2Np_+^2 p_-^2 & \text{for } i = 0, j = 1, \text{ and vice versa} \\ 2p_+^2 & \text{for } i = 0, j = 3N/2 + 1, \text{ and vice versa} \\ p_+^2 & \text{for } i = 0, j \geq 2 (j \neq 3N/2 + 1), \text{ and vice versa} \\ 2p_-^2 & \text{for } i = 1, j = 3N/2 + 1, \text{ and vice versa} \\ p_-^2 & \text{for } i = 1, j \geq 2 (j \neq 3N/2 + 1), \text{ and vice versa} \end{cases}$$

For $2 \leq i \leq 2N$ and $2 \leq j \leq 2N$

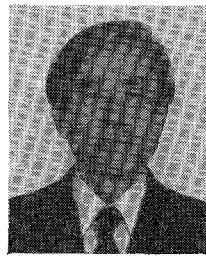
$$\frac{\theta_{ij}}{\theta} = \begin{cases} 3/(8N) & \text{for } i = j, i \neq \nu N/4 + 1 (\nu = 0, 1, \dots, 7) \\ 0 & \text{for } i = N/2 + 1, j \geq 2, \text{ and vice versa} \\ 1/N & \text{for } i = 3N/2 + 1, j \geq 2 (j \neq N/2 + 1), \text{ and vice versa} \\ 3/(4N) & \text{for } i - j = \pm 3N/2 (j \neq \tilde{i}) \\ & i + j - 2 = N (i - j \neq \pm N/2, i \neq 2 + 1) \\ & i + j - 2 = 3N (i - j \neq \pm N/2, i \neq 3N/2 + 1) \\ & i - j = \pm 3N/4, \pm 5N/4 \\ & i + j - 2 = 3N/2, 5N/2 \\ & i - j = \pm N, i + j - 2 = 7N/4, 9N/4. \\ 1/(4N) & \text{for } j = \tilde{i}, i \neq \nu N/4 + 1 (\nu = 1, 2, 3, 5, 6, 7, \\ & i + j - 2 = N/2, 7N/2 \\ & i = j = \nu N/4 + 1 (\nu = 1, 3, 4, 5, 7) \\ & i - j = \pm N, j \neq \tilde{i}, i + j - 2 \neq 3N/2, 5N/2 \\ & i + j - 2 = 3N/2, 5N/2, i - j = \pm N/4 \\ & i - j = \pm N/2, i + j - 2 = \nu N/4 (\nu = 3, 5, 11, 13) \\ 1/(2N) & \text{for other } (i, j)'s. \end{cases}$$

$$\frac{\xi_{i\tilde{i}j\tilde{j}}}{\theta} = \begin{cases} -1/(4N) & \text{for } (i, j) = (N/4 + 1, \nu N/4 + 1) (\nu = 3, 5) \\ & (i, j) = (7N/4 + 1, \nu N/4 + 1) (\nu = 3, 5) \\ & \text{and vice versa} \\ 0 & \text{for other } (i, j)'s. \end{cases}$$

- [5] K. Fukui and S. Nogi, "Power combining ladder network with many active devices," *IEEE Trans. Microwave Theory Tech.*, vol. MTT-28, pp. 1059-1067, Oct. 1980.
- [6] S. Nogi and K. Fukui, "Optimum design and performance of a microwave ladder oscillator with many diode mount pairs," *IEEE Trans. Microwave Theory Tech.*, vol. MTT-30, pp. 753-743, May 1982.
- [7] T.-E. Ma and C. Sun, "1-W millimeter wave Gunn diode combiner," *IEEE Trans. Microwave Theory Tech.*, vol. MTT-28, pp. 1460-1463, Dec. 1980.
- [8] A. Materka and S. Mizushima, "A waveguide-cavity multiple-device FET oscillator," *IEEE Trans. Microwave Theory Tech.*, vol. MTT-30, pp. 1237-1241, Aug. 1982.
- [9] M. Madhian and S. Mizushima, "A 3M-device cavity-type power combiner," *IEEE Trans. Microwave Theory Tech.*, vol. MTT-31, pp. 731-735, Sept. 1983.
- [10] R. S. Harp and H. L. Stover, "Power combining of X-band IMPATT circuit modules," in *1973 IEEE-ISSCC Dig.*, vol. XVI, Feb. 1973, pp. 118-119.
- [11] R. Aston, "Techniques for increasing the bandwidth of a TM_{010} -mode power combiner," *IEEE Trans. Microwave Theory Tech.*, vol. MTT-27, pp. 479-482, May 1979.
- [12] M. Dydyk, "Efficient power combining," *IEEE Trans. Microwave Theory Tech.*, vol. MTT-28, pp. 755-762, July 1980.
- [13] C. A. Drubin, A. L. Hieber, G. Jerinic, and A. S. Marinilli, "A 1 kW_{peak} , 300W_{avg} IMPATT diode injection locked oscillator," in *1982 IEEE MTT-S Symp. Dig.*, May 1982, pp. 126-128.
- [14] K. Fukui, S. Nogi, and T. Sato, "Stable power-combining mode operation of a cylindrical cavity multiple-device oscillator," *Trans. IECEJ*, vol. J68-B, pp. 1011-1019, Sept. 1985 (in Japanese).
- [15] M. Kuramitsu and F. Takase, "An analytical method for multi-mode oscillators using the averaged potential," *Trans. IECEJ*, vol. J66-A, pp. 336-343, Apr. 1983 (in Japanese). Also, M. Kuramitsu and F. Takase, "The analysis of the square array of van der Pol oscillators using the averaged potential," *Int. J. Nonlinear Mechanics*, vol. 20, pp. 395-406, May 1985.
- [16] N. Kryloff and N. Bogoliuboff, *Introduction to Nonlinear Mechanics*. Princeton Univ. Press, 1949.
- [17] S. Nogi and K. Fukui, "Cylindrical cavity multiple-device oscillator/power amplifier of window output," IECE Japan, Tech. Rep. MW85-9, May 1985 (in Japanese).

*

Kiyoshi Fukui (M'75) was born in Tokushima Prefecture, Japan, on January 13, 1930. He received the B.Sc. degree in physics in 1952 and the D.Eng. degree in electronics engineering in 1964, both from Kyoto



University, Kyoto, Japan.

From 1958 to 1962, he was a Research Assistant at the Department of Electronics, Kyoto University. From 1962 to 1967, he taught as an Assistant Professor at the Training Institute for Engineering Teachers, Kyoto University. In 1967, he became a Professor of Electronics at the Himeji Institute of Technology, Himeji, Japan. Since 1971, he has been with the Department of Electronics, Okayama University. During 1977-1978, he was a Visiting Professor at the University of Wisconsin-Madison. His research interest has been mainly in nonlinear phenomena in electronics, such as locking phenomena in oscillators, frequency multiplication by variable capacitance, behavior of multiple-device structures, and nonlinear wave propagation.

Dr. Fukui is a member of the Institute of Electronics and Communication Engineers of Japan and the Physical Society of Japan.

*



Shigeji Nogi was born in Osaka Prefecture, Japan, on December 26, 1945. He received the B.E., M.E., and D.Eng. degrees in electronics engineering from Kyoto University, Kyoto, Japan, in 1968, 1970, and 1984, respectively.

From 1970 to 1972, he was employed by the Central Research Laboratory, Mitsubishi Electronic Corporation, Amagasaki, Japan. In 1972, he joined the Department of Electronics, Okayama University, where he has been engaged in research on microwave active circuits, multi-mode oscillators, and nonlinear wave propagation.

Dr. Nogi is a member of the Institute of Electronics and Communication Engineers of Japan.